

59-33

160523

N93-27735

## THERMIONIC EMISSION CURRENT IN A SINGLE BARRIER VARACTOR

Hans Hjelmgren<sup>a)</sup>, Jack East<sup>b)</sup>, and Erik Kollberg<sup>a)</sup>

a) Applied Electron Physics, Chalmers University of Technology, S-412 96 Göteborg, Sweden

b) Solid-State Electronics Laboratory, University of Michigan, Ann Arbor, MI 48109-2122

*Abstract*—From I–V measurements on Single Barrier Varactors (SBV) at different temperatures we concluded that thermionic emission across the barrier of the actual device is mainly due to transport through the X band. The same structure was also modelled with a one-dimensional drift-diffusion model, including a "boundary condition" for thermionic emission across the heterojunction interface. By including thermionic field emission through the top of the triangular barrier of a biased diode and the effect of a non-abrupt interface at the heterojunction, we obtained good agreement between the modelled and measured I–V characteristics.

### 1. Introduction

SBV diodes have been proposed as an alternative to Schottky barrier diodes for harmonic multiplier applications [1]. However, the device discussed in [1] showed a higher than expected current. We will present experimental data and the results of a numerical model to explain the current vs. voltage characteristics of SBV diodes.

### 2. Experimental results

The device consists of a 200 Å wide undoped  $\text{Al}_{0.7}\text{Ga}_{0.3}\text{As}$  barrier, surrounded by 5300 Å wide GaAs layers, doped to  $1 \times 10^{17} \text{ cm}^{-3}$ . On both sides of the AlGaAs layer there is a 50 Å wide undoped GaAs spacer layer. If the effect of field emission is neglected the current is mainly limited by thermionic emission across the barrier and can be described by the Richardson law,

$$J = A^* T^2 e^{-\phi_b / kT} \quad (1)$$

where  $A^*$  is the modified Richardson constant and  $\phi_b$  is the bias dependent barrier height. Both can be determined from the experimental data by plotting  $\ln(J/T^2)$  against  $1000/T$  for different voltages [2]. The intersection with the y-axis gives us the Richardson constant, while the slope is proportional to the barrier height for that specific bias voltage. Since our barrier is comparatively thin, the influence of tunneling is observable even at quite high temperatures, causing a deviation from a straight line in Fig. 1. This makes the determination of the Richardson constant quite cumbersome. It must be chosen in such a way that the barrier heights at low voltages are close to the expected barrier height at zero bias voltage. A Richardson constant of  $0.30 \text{ A cm}^{-2} \text{ K}^{-2}$ , much lower than the value expected for thermionic emission in GaAs but in fairly good agreement with that measured by Solomon et al. [2], corresponds to a barrier height at low voltages of about 0.29 eV. This low Richardson constant together with the high current indicates that the electrons are transferring to the X valley within the barrier. The assumed offset in  $\Gamma$  conduction band corresponds to 59 % of the difference in bandgap [3].

### 3. Numerical results

A drift-diffusion model for one-dimensional heterojunction structures was also used to study the device characteristics. It accounts for thermionic emission across the barrier by calculating the current at the heterojunction interfaces from,

$$J = q\eta_2 n_2 v_{r2} - A^* T^2 e^{-\phi_b(V)/kT} \quad (2)$$

where the first term describes the current from the AlGaAs side [4] while the second term is the current from the GaAs side emitted above the barrier. Without this "bottleneck" for the current, the drift-diffusion model results in a much too high current. Since a theoretical determination of the actual emission constant across the interface is quite complicated, we have used the experimentally determined Richardson constant in Fig. 1. The probability of emission above the barrier depends on several parameters, such as thickness of the barrier, crystal orientation, and roughness of the interfaces. The thermally emitted electrons were assumed to be transferred to the X-valley when they reached the AlGaAs barrier, causing an effective barrier height at zero bias of 0.29 eV. During a simulation the barrier height is determined self consistently from the modelled conduction band, Fig. 2. Even at 300 K the effect of thermally assisted tunneling is considerable, and it has to be included in the model. Since the top of the biased barrier is triangular, the probability of tunneling as a function of electric field and carrier energy can be estimated from the WKB approximation [5],

$$P = \exp \left\{ - \frac{4\sqrt{2q m_e} \Delta e^{3/2}}{3(h/2\pi) E_{\max}} \right\} \quad (3)$$

where  $E_{\max}$  is the electric field in the barrier and  $\Delta e$  is the energy distance from the top of the barrier. The effect is included in the model by reducing the barrier height in eqn. (2) with an amount  $\Delta e$  corresponding to a tunnelling probability of  $e^{-1}$ . We assumed the tunneling process to be indirect tunneling in the AlGaAs X band [6], and used a transverse electron mass in the X band of  $0.20m_0$ . Tunneling through the  $\Gamma$  band is less probable due to the much higher barrier, and tunneling from X valleys with the longitudinal mass perpendicular to the interface is less probable due to the higher mass. Apart from band bending due to accumulation of electrons at the interface, and thermionic field emission, the fact that the transition between the two materials is not completely abrupt will also result in a field dependent barrier height [7]. In Fig. 2 we roughly modelled this effect by using a grid distance of 25 Å at the interface. The obtained I-V characteristic in Fig. 3 is very sensitive to the grid distance at the right interface of the barrier, while its value elsewhere is of less importance.

The model has also been used to predict the capacitance vs. voltage. The capacitance is determined from the change of charge concentration in the depletion layer for an incremental change in voltage. As can be seen in Fig. 4, the agreement between modelled and measured C-V characteristics is fairly good. In order to get reasonably good accuracy the grid-distance in the depletion layer and the voltage step should not be too large.

### 4. Conclusions

The presented expression for the current between the two grid-points adjacent to the heterojunction interface (eqn. 2) includes effects caused by the existence of two interfaces and other effects, which for a theoretical determination require quantum mechanical calculations [8]. It also gives us a possibility to model the effect of a non-abrupt transition between the two materials. Similar expressions, have been used before in drift-diffusion models, but they are restricted to a single interface [3,4]. The drawback with the model used here is that it relies on measured results in order to find a value for the Richardson

emission constant. However, since the actual emission constant may be quite difficult to calculate, we considered it as a device parameter specific for the actual device dimensions and growing conditions, which could be measured instead of calculated. The good agreement with measured results indicates that the current is mainly due to thermionic emission and thermionic field emission across the X-valley of the barrier.

The inaccuracy in the experimental determination of the Richardson constant can be reduced by using slightly thicker barriers and by performing measurements at elevated temperatures and lower bias voltages.

#### References

1. A. Rydberg, H. Grönqvist, and E. Kollberg, "Millimeter- and submillimeter-wave multipliers using quantum-barrier-varactor (QBV) diodes," *IEEE El. Device Lett.*, vol. 11, pp. 373–375, 1990.
2. P. Solomon, S. Wright, and C. Lanza, "Perpendicular transport across (Al,Ga)As and the  $\Gamma$  to X transition," *Superlattices and Microstructures*, vol. 2, pp. 521–525, 1986.
3. G. B. Tait and C. R. Westgate, "Electron transport in rectifying semiconductor alloy ramp heterostructures," *IEEE Trans. Electron Devices*, vol. 38, pp. 1262–1270, 1991.
4. K. Horio and H. Yanai, "Numerical modeling of heterojunctions including the thermionic emission mechanism at the heterojunction interface," *IEEE Trans. Electron Devices*, vol. 37, pp. 1093–1098, 1990.
5. E. H. Rhoderick and R. H. Williams, "Metal–Semiconductor Contacts, 2nd edition," Oxford, England: Clarendon, 1988.
6. E. E. Mendez, E. Calleja, and W. L. Wang, "Tunneling through indirect-gap semiconductor barriers," *Physical Rev. B*, vol. 34, pp. 6026–6029, 1986.
7. S. C. Lee and G. L. Pearson, "Rectification in  $\text{Al}_x\text{Ga}_{1-x}\text{As}$ –GaAs N–n heterojunction devices," *Solid-State Electronics*, vol. 24, pp. 561–568, 1981.
8. M. Rossmanith, J. Leo, and K. von Klitzing, "Model of  $\Gamma$  to X transition in thermally activated tunnel currents across  $\text{Al}_x\text{Ga}_{1-x}\text{As}$  single barriers," *J. Appl. Phys.*, vol. 69, pp. 3641–3645, 1991.

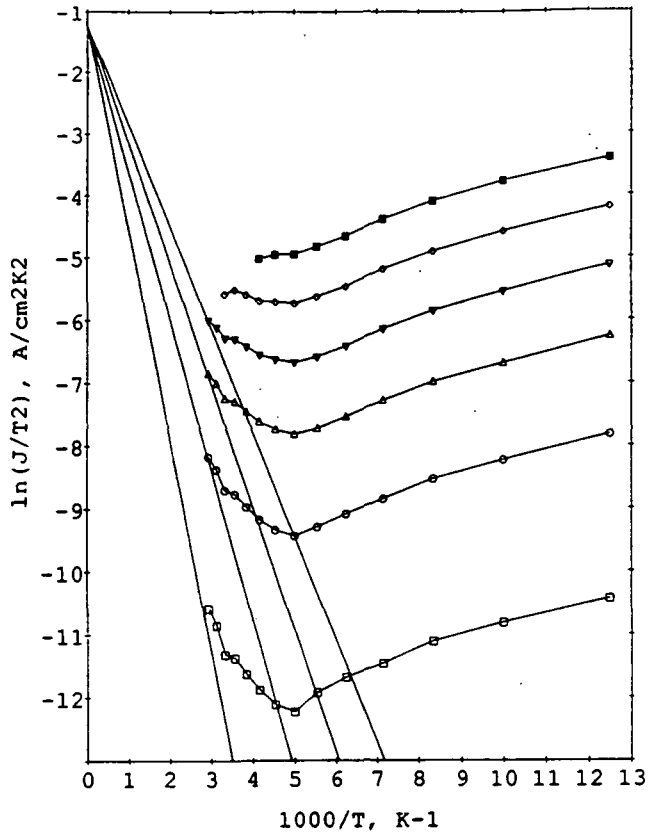


Fig. 1. Plotting of experimental data in a  $\ln(J/T^2)$  vs.  $1000/T$  diagram. The applied voltages are 0.1 V, 0.5 V, 1.0 V, 1.5 V, 2.0 V, and 2.5 V (filled squares).

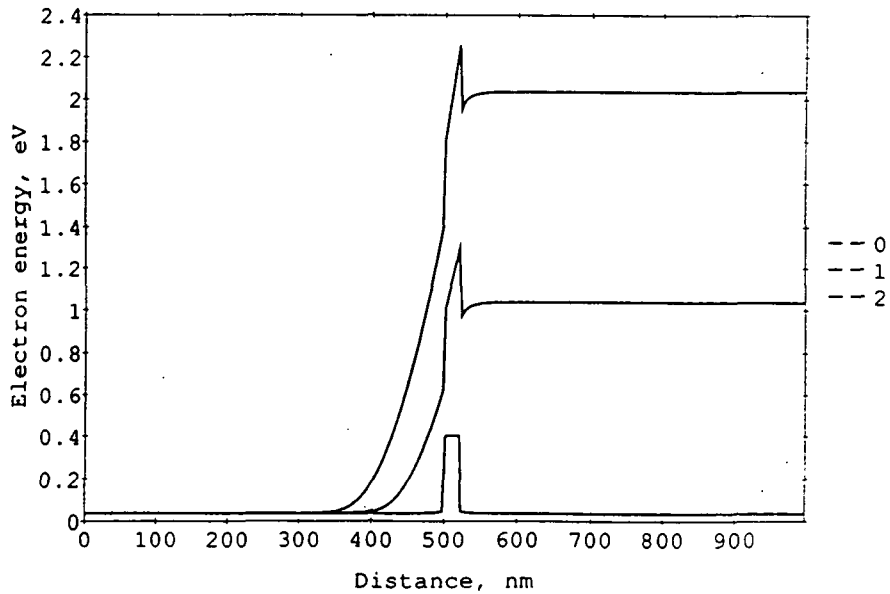


Fig. 2. Simulated conduction bands for different applied voltages (0.0 V, 1.0 V, and 2.0 V).

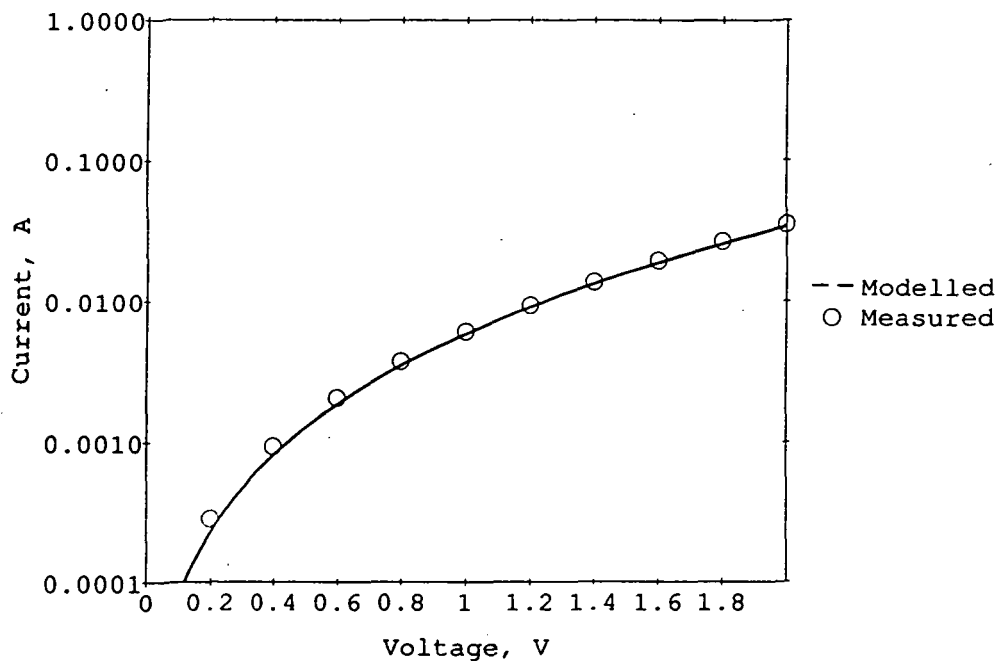


Fig. 3. Comparison between modelled and measured I-V characteristics at 300 K. The effects of thermally assisted tunneling and a nonabrupt heterojunction interface are included in the simulation.

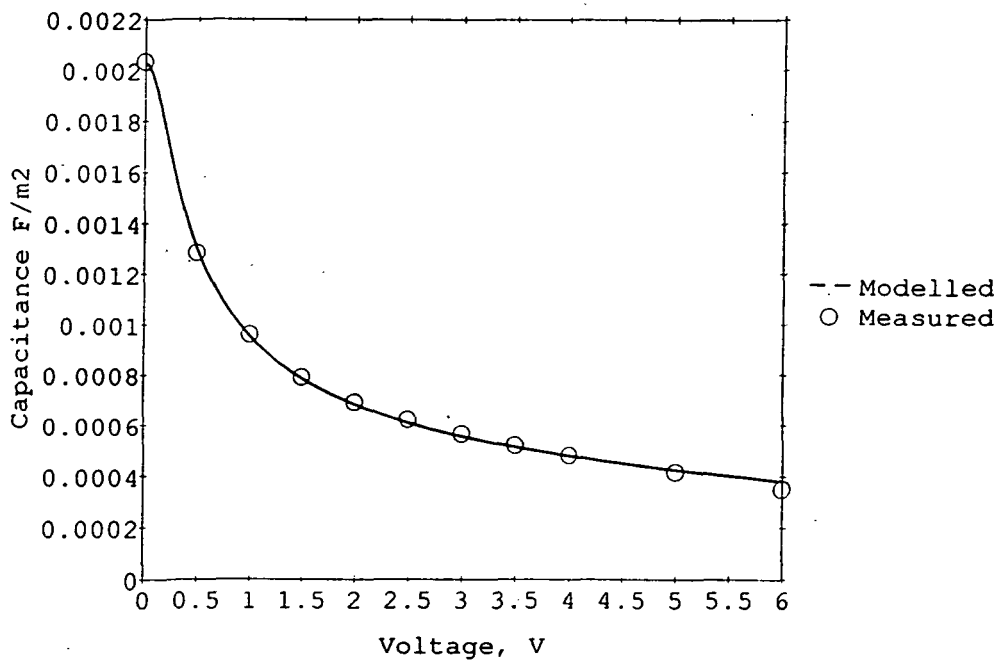


Fig. 4. Comparison between modelled and measured C-V characteristics at 300 K.